J|A|C|S
ARTICLES
Published on Web 01/04/2003

Molecular Quantum-Dot Cellular Automata

Craig S. Lent,* Beth Isaksen,† and Marya Lieberman‡

Contribution from the Center for Nano Science and Technology, Department of Electrical Engineering, and Department of Chemistry and Biochemistry, University of Notre Dame, Notre Dame, Indiana 46556

Received May 10, 2002; E-mail: lent@nd.edu

Abstract: Molecular electronics is commonly conceived as reproducing diode or transistor action at the molecular level. The quantum-dot cellular automata (QCA) approach offers an attractive alternative in which binary information is encoded in the configuration of charge among redox-active molecular sites. The Coulomb interaction between neighboring molecules provides device−device coupling. No current flow between molecules is required. We present an ab initio analysis of a simple molecular system which acts as a molecular QCA cell. The intrinsic bistability of the charge configuration results in dipole or quadrupole fields which couple strongly to the state of neighboring molecules. We show how logic gates can be implemented. We examine the role of the relaxation of nuclear coordinates in the molecular charge reconfiguration.

Quantum-Dot Cellular Automata

Computers dating back to those composed of electromechanical relay switches have relied on encoding binary information in the on or off state of a current switch. While this has been remarkably successful, it may not be the appropriate paradigm for realizing single-molecule devices. An alternative approach, quantum-dot cellular automata (QCA),[1] parallels conventional computing in using a binary representation of information (not qubits) yet realizes functionality in ways which are well-suited to the properties of single molecules − using molecules not as current switches but as structured charge containers. Binary information is encoded in the charge configuration of a cell composed of a small number of quantum "dots". A dot for these purposes is simply a region in which charge is localized. Each cell has two extra mobile electrons and in isolation has two degenerate ground states. The electrostatic effect of neighboring cells lifts the degeneracy and results in a "1" or "0" state of the cell. This intercellular interaction involves no current flow between cells. Remarkably, this interaction is sufficient to enable a general purpose computation.[2]

Figure 1a illustrates a schematic four-dot QCA cell (several variations are possible). The electrons naturally ocupy antipodal sites. Note that the full four-dot cell can also be viewed as a pair of half-cells (with two dots each) in which the sign of the dipole alternates. Juxtaposing cells in a linear array, as in Figure 1b, result in a QCA wire, which can transmit binary information from one end to the other. The natural logic gate in this approach is the three-input majority gate shown in Figure 1c. The three input lines converge at a device cell, whose state is determined by the state of the majority of the inputs. Building up from these, we have designed more complex circuits such as adders[2] and even simple microprocessors[3] within the QCA paradigm.

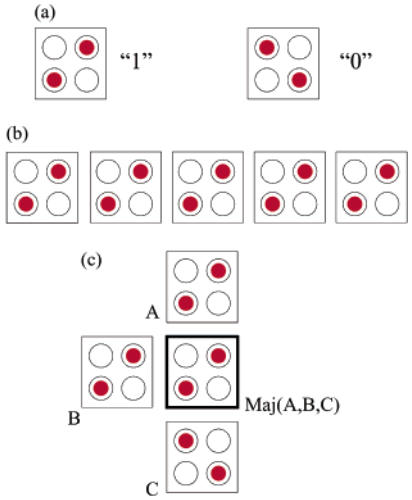

Figure 1. (a) Schematic of QCA cells. Coulomb repulsion keeps the electrons, shown in red, at antipodal sites. A "1" or "0" bit is encoded in the arrangement of charge. (b) A QCA wire is formed by a linear array of cells. Electrons do not move from cell to cell, but the intercellular Coulomb interaction makes it energetically favorable for all of the cells to have the same state. (c) A QCA majority logic gate consists of three inputs (which may come from other wires) which converge on a device cell. The state of the cell is determined by the state of the majority of the inputs.

QCA devices using single electron switching have been demonstrated using small metallic dots at low temperatures.[4] In these devices, the role of the dot is played by a small metal island connected to other islands by small tunnel-junction

† Department of Electrical Engineering.
‡ Department of Chemistry and Biochemistry.

(1) Lent, C. S.; Tougaw, P. D.; Porod, W.; Bernstein, G. H. *Nanotechnology* **1993**, *4*, 49.
(2) Lent, C. S.; Tougaw, P. D. *Proc. IEEE* **1997**, *85*, 541.
(3) Niemier, M. T.; Kogge, P. M. *Int. J. Circuit Theory Appl.* **2001**, *29*, 49.
(4) (a) Orlov, A. O.; Amlani, I.; Bernstein, G. H.; Lent, C. S.; Snider, G. L. *Science* **1997**, *277*, 928. (b) Amlani, I.; Orlov, A.; Toth, G.; Bernstein, G. H.; Lent, C. S.; Snider, G. L. *Science* **1999**, *284*, 289.

10.1021/ja026856g CCC: $25.00

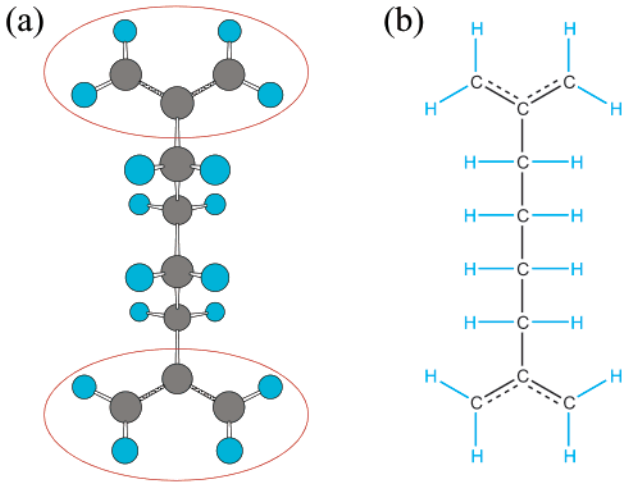

Figure 2. Two views of molecule **1**. The p-system of the allyl end-groups has nonbonding levels which play the role of dots for QCA. We consider the molecular cation for which one allyl group is neutral and the other is a radical cation.

barriers. The tunnel junctions act as capacitors which couple the potential on one dot to that of others and provide a path for quantum-mechanical tunneling. These experiments have shown that indeed the rearrangement of single charges in one cell can effectively change the state of neighboring cells and perform computational tasks. Majority logic gates, wires, memories, and clocked shift-registers have all been demonstrated. This QCA scheme has two potentially significant advantages over other approaches: power dissipation can be greatly reduced, and true power gain is possible.[5]

Molecular QCA

A single-molecule implementation of a QCA cell requires a molecule in which charge is localized on specific sites and can tunnel between those sites.[6] The role of the dots is then played by redox sites, with tunneling paths provided by bridging ligands. While many candidate molecular systems have been discussed, and several are under active experimental investigation,[7] we focus here on a particularly simple molecule, **1**, shown in Figure 2, first proposed by Aviram[8] and later studied by Hush et al.[9] The context in which this molecule was then examined was primarily as a gate for molecular current switches. Aviram called attention to the possibilities of electron localization in the allyl π-system in the end-groups, and the tunneling barrier created by the σ-bonded bridge. We here explore its utility as a prototype system for molecular QCA.

It should be stated at the outset that **1** serves us here, as it did for Aviram and Hush, as a model system offering computational tractability while displaying key features of more complex mixed-valence systems. Practical QCA molecules would require more than this molecule can offer. Functional groups that allow attachment and orientation on a surface would be required. A means of setting and reading molecular states at the edge of the molecular arrays is necessary for input/output. Stable, neutral species would be helpful in eliminating the need for counterions. Moreover, many of the benefits of QCA architectures derive from the ability to have clocked control of the effective tunnel barriers between dots. Each of these represent important challenges, and possible solutions are being explored in molecules more complex than **1**. Here, however, we will not address questions of layout and patterning, input/output, appropriate circuit architecture, clocked control, or the speed of switching response. As was the experience with the metal-dot implementations, the first step is establishing the basic character of a nonlinear, bistable interaction between molecules, on which the essential device performance depends.

Molecule **1** (1,4-diallyl butane radical cation) consists of two allyl groups connected by a butyl bridge. We are interested in the molecular cation for which one allyl group is a neutral radical and the other is cationic (the molecular anion behaves very similarly). The three-carbon π-system in the allyl group has a doubly occupied bonding level and a nonbonding level which is singly occupied in the neutral allyl radical and unoccupied in the allyl cation. The unpaired electron can occupy either of the nonbonding levels at the opposite allyl end-groups with little change to the molecular geometry. This system provides an example of localized states with nonbonding character which can play the role of dots for QCA. If the charge is resident in one end but not the other, the molecule will develop a dipole moment, which changes sign when the electron tunnels from one end to the other. Because the charged end has one *less* electron than does the neutral end, it will be helpful to view this process as a hole tunneling from one allyl end-group to the other. QCA action is possible because, as we will show, the dipole field from one molecule can cause the dipole moment of a neighboring molecule to change sign. That is, the charge configuration of one molecule (=QCA cell) is coupled to the charge configuration of its neighbor.

Ab Initio Calculations. All calculations reported here were performed with Gaussian 98[10] using unrestricted Hartree−Fock theory and the STO-3G basis set. This theory level was used by Aviram[8] and Hush[9] and offers the advantage of computational tractability. Improvements in computational power since those two studies allow us to solve for the molecule as a whole in a variety of conditions, rather than optimizing components separately. Higher levels of accuracy are not crucial to the present discussion because we are interested in the gross features of how charges respond to changes in the local field due to neighboring molecules in what is admittedly a simplified model system.[11]

The ground-state relaxed geometry of molecule **1** was calculated. A systematic study of the low-energy conformation

(5) Timler, J.; Lent, C. S. *J. Appl. Phys.* **2002**, *91*, 823.
(6) Lent, C. S. *Science* **2000**, *288*, 1597.
(7) Lieberman, M. L.; Chellamma, S.; Varughese, B.; Wang, Y.; Lent, C. S.; Bernstein, G. H.; Snider, G.; Peiris, F. C. *Ann. N.Y. Acad. Sci.* **2002**, *960*, 225.
(8) Aviram, A. *J. Am. Chem. Soc.* **1988**, *110*, 5687.
(9) Hush, N. S.; Wong, A. T.; Backskay, G. B.; Reimers, J. R. *J. Am. Chem. Soc.* **1990**, *112*, 4192.
(10) Frisch, M. J.; Trucks, G. W.; Schlegel, H. B.; Scuseria, G. E.; Robb, M. A.; Cheeseman, J. R.; Zakrzewski, V. G.; Montgomery, J. A.; Stratmann, R. E.; Burant, J. C.; Dapprich, S.; Milliam, J. M.; Daniels, A. D.; Kudin, K. N.; Strain, M. C.; Farkas, O.; Tomasi, J.; Barone, V.; Cossi, M.; Cammi, R.; Mennucci, B.; Pomelli, C.; Adamo, C.; Clifford, S.; Ochterski, J.; Petersson, G. A.; Ayala, P. Y.; Cui, Q.; Morokuma, K.; Malick, D. K.; Rabuck, A. D.; Raghavachari, K.; Foresman, J. B.; Cioslowski, J.; Ortiz, J. V.; Stefanov, B. B.; Liu, G.; Liashenko, A.; Piskorz, P.; Komaromi, I.; Gomberts, R.; Martin, R. L.; Fox, D. J.; Keith, T. A.; Al-Laham, M. A.; Peng, C. Y.; Nanayakkara, A.; Gonzalez, C.; Challacombe, M.; Gill, P. M. W.; Johnson, B. G.; Chen, W.; Wong, M. W.; Andres, J. L.; Head-Gordon, M.; Replogle, E. S.; Pople, J. A. *Gaussian 98*, revision A.11; Gaussian Inc.: Pittsburgh, PA, 2001.
(11) Local density approaches typically underestimate the degree of charge localization. Hartree−Fock may overestimate localization somewhat. A comparison of different methods would need to be benchmarked against experiments and is beyond the scope of this work.

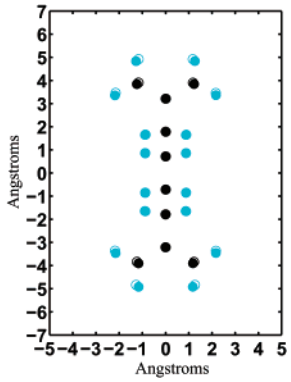

Figure 3. Molecular relaxation. The projected coordinates are shown for molecule **1** (same view as Figure 2a). Open circles represent the **1**-PLUS state for which the unpaired electron is in the bottom allyl group and the dipole moment points up. Solid circles show the configuration for the **1**-MINUS state for which the unpaired electron is in the top allyl group and the dipole moment points down.

was made, examining carefully the structure of the butyl bridge and the energetics of the orientation of the allyl planes. The optimal geometry, shown in Figure 2, has four coplanar carbons in the bridge, with both allyl groups in planes perpendicular to that of the bridge.

The molecular radical cation has two degenerate ground-state conformations, with charge localized on either the top or the bottom allyl end-group. We refer to the state with a positive dipole moment[12] as **1**-PLUS. For this state, the unpaired electron is on the bottom allyl group, and the positive charge is on the top allyl group. The state with a negative dipole moment, positive charge on the bottom group and electron on the top group, we call the **1**-MINUS configuration. The charge state of the allyl ends is coupled to a relaxation of the nuclear positions. The relaxation amounts to a slight spreading out of the neutral allyl end and contraction of the cationic end, as shown in Figure 3. In addition to the two optimized structures, we calculate a symmetric transition state structure, **1**-SYM, for which the nuclear coordinates are intermediate between **1**-MINUS and **1**-PLUS. The **1**-SYM is geometrically symmetric, favoring electron occupation of neither the top nor the bottom allyl group. In that case, the HOMO is delocalized over both ends of the molecule. Figure 4 shows the calculated HOMO for each of these three configurations.

Single-Molecule Response

A key requirement for QCA operation is that the molecular charge distribution respond in a nonlinear way to the Coulombic perturbation produced by a neighboring molecule switching from one state to another. The switching of the state of a single electron must be sufficient to switch the state of another electron. The Coulomb field produced by the neighboring molecules can be considered the input to the molecular device, and the resulting charge configuration can be considered as its output.

We model the input as a unit point charge, here a hole, which moves on a line parallel to the molecular axis (the center line of the butyl bridge) as shown in Figure 4d. The driver is 7 Å from the molecular axis, to provide a roughly square geometry, and the positions of the two central carbon atoms in the bridge

(12) We take the direction of the dipole moment to be from negative to positive charge, following: Stone, A. J. *The Theory of Intermolecular Forces*; Oxford University Press: Oxford, 1996.

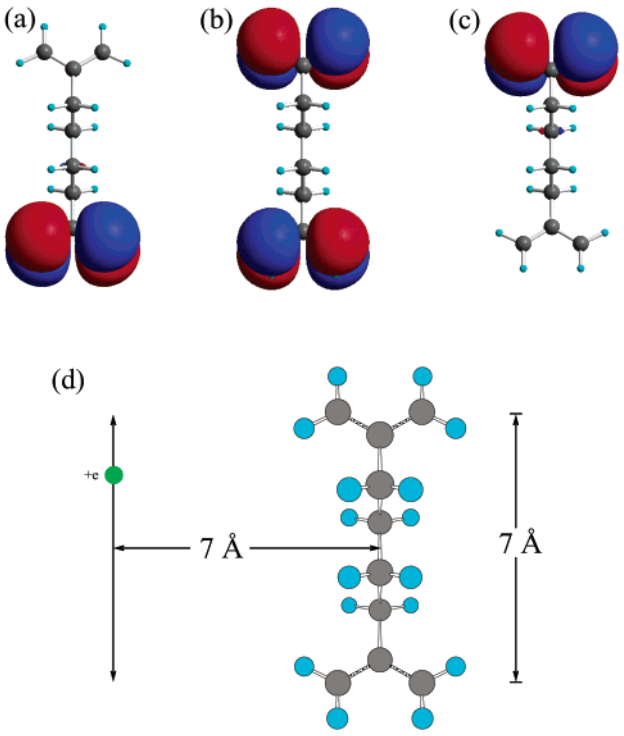

Figure 4. (a) HOMO for the **1**-PLUS state for which the unpaired electron is in the bottom allyl group. (b) HOMO for the **1**-SYM transition state structure for which the nuclear geometry is precisely symmetric. In this case, the unpaired electron is in a delocalized state. (c) HOMO for the **1**-MINUS state for which the unpaired electron is in the top allyl group. (d) Driver geometry. The effect of a nearby molecule is simulated by a single positive unit charge moving on the axis parallel to the molecular axis as shown.

are held fixed. This admittedly artificial driver model will be justified by the response of the molecule itself.

We are interested in the electronic response to this driver, which presents a varying dipole moment to the molecule. Figure 5a shows the calculated molecular dipole moment μ_{molecule} of **1**, along the molecular axis, as a function of the dipole moment of the driver μ_{driver}. Data shown as circles represent the induced dipole moment when the geometry is held fixed in the **1**-SYM configuration. Data represented by squares correspond to the induced dipole moment when, for each value of the driver, the molecule is allowed to relax its nuclear coordinates. We can think of this as a two-stage process: the driver field pushes the electron (or hole) to one end or the other, and then the nuclear coordinates relax around the new electronic configuration. This nuclear relaxation acts as a kind of "self-trapping" mechanism, which further stabilizes the molecular dipole. The induced dipole moment μ_{molecule} is essentially unchanged by this nuclear relaxation. The results for the frozen **1**-SYM structure are important because they illustrate that the bistability of the charge configuration is present in the *electronic* structure of the molecule − it is not simply the result of the nuclear relaxation.

The nonlinearity evident in the response curve shown in Figure 5a is ideal for QCA operation. Even a small driver dipole moment induces a large dipole moment in the molecule. This nonlinear response plays the role of voltage gain in conventional devices (power gain in QCA has recently been analyzed[5]). Viewed as a device transfer function−output signal versus input signal, Figure 5a corresponds to that of a high-gain inverter. A first approximation to the response of a chain of such molecular

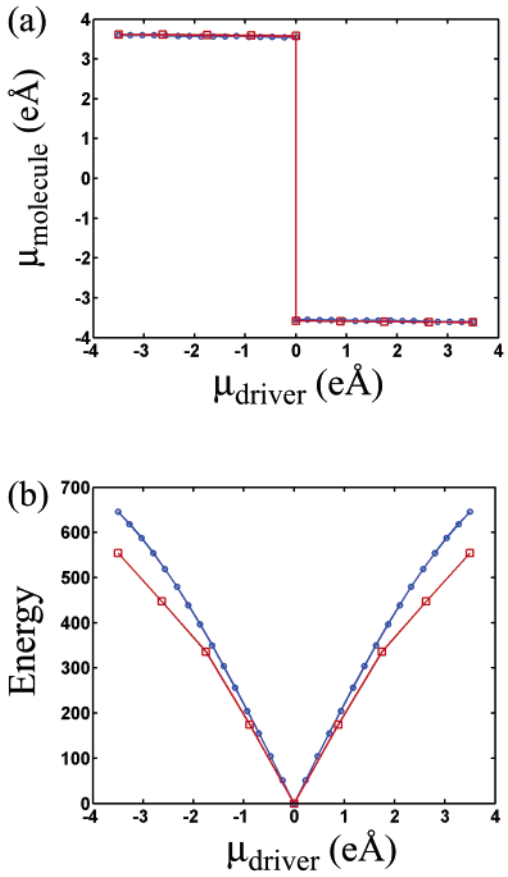

Figure 5. Molecular QCA response. (a) The response function of **1** when driven by the driver shown in Figure 4d. For each driver dipole moment, the induced molecular dipole moment is calculated. Blue circles are for the case of a nuclear geometry frozen in the **1**-SYM configuration. Red squares are obtained by letting the molecule relax to its equilibrium position in the presence of the driver. The nonlinear bistable response corresponds to that of a high-gain inverter. (b) The excitation energy (in meV) from the ground state to the first excited "mistake" state as a function of driver moment.

cells is obtained by iterating the transfer function, which here would result in a fully saturated inverter chain. Each molecular dipole would induce the opposite dipole in its neighbor.[13]

In addition to the transfer function, it is important to find the excitation energy of a molecular QCA device. The driver dipole induces a molecular ground state with a dipole moment which is *anti-aligned* with the driver. The molecular state with a dipole moment *aligned* with the driver is an excited state of the molecule with an energy $\Delta E(\mu_{\text{driver}})$ above the ground state.

We calculate the energy ΔE approximately by the following simple technique. We use as initial guesses for the SCF iteration molecular electronic configurations **1**-PLUS and **1**-MINUS (in addition to Gaussian 98's default). The "right" initial guess (that is anti-aligned with the driver) invariably results in the lowest energy converged solution. The "wrong" initial guess converges to a higher-energy state, which approximates to the excited state of the molecule.[14] Figure 5b shows the energy difference $\Delta E(\mu_{\text{driver}})$ between the ground state and the first excited "mistake" state as a function of the driver dipole. Again, curves

(13) Recall that we are concerned here with the ground-state configuration, not with the temporal response and switching transient.

(14) Although the Hartree−Fock self-consistent iteration is not guaranteed to produce the right excited state, in this case, the energy difference is dominated by the electrostatic interaction with the driver (see below), so it provides a reasonable approximation to the excitation energy.

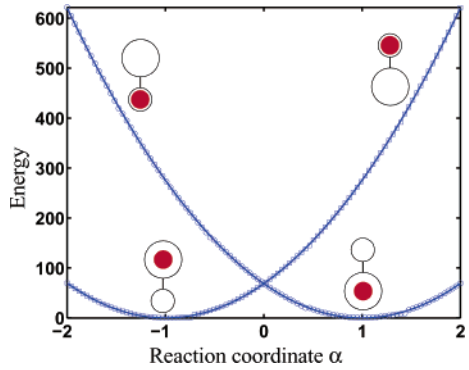

Figure 6. The calculated total energy (in meV) is plotted as a function of reaction coordinate a, which corresponds to nuclear motion between the **1**-PLUS ($a = 1$) and **1**-MINUS ($a = -1$) states of Figure 3. The ground-state double-well curve illustrates the role of self-trapping in stabilizing the bistability of the charge distribution. A barrier of 68 meV separates the two configurations. The position of the unpaired electron (red dot) and the relaxation of the allyl group geometry are shown schematically in the small figures. No driver is present.

are shown for the case when the nuclear motion is frozen in the **1**-SYM state (○) and when it is allowed to relax to its equilibrium state (□).

Role of Nuclear Relaxation. The molecular electronic configuration is coupled to the nuclear degrees of freedom. When **1** switches its dipole moment (a hole tunneling from one end to the other), there is a related relaxation of the nuclear positions which changes the structure from (say) the **1**-PLUS to **1**-MINUS configurations. The relation between the energies associated with the electronic rearrangement and the corresponding nuclear relaxation has led to the classification of such mixed-valence compounds into the classes of Robin and Day.[15] We examine the energetics of electron transfer coupled to the **1**-PLUS to **1**-MINUS transition including, importantly, the effect of the driver.

The nuclear coordinates for configurations **1**-PLUS and **1**-MINUS are denoted $\{R_i^+\}$ and $\{R_i^-\}$, where i runs over the atoms in the molecule. We define a reaction coordinate α which connects the positive and negative dipole states. The nuclear coordinates of intermediate states are written

$$R_i(\alpha) = \left(\frac{1+\alpha}{2}\right)R_i^+ + \left(\frac{1-\alpha}{2}\right)R_i^- \qquad (1)$$

The state **1**-SYM has, by definition, nuclear coordinates $\{R_i^{\text{SYM}} = R_i(\alpha = 0)\}$. For each value of α, the total energy is calculated using both **1**-PLUS and **1**-MINUS electronic states as initial guesses. Plotting $E(\alpha)$ results in the energy-coordinate diagram shown in Figure 6. This double-well diagram, familiar in the literature of mixed-valence compounds,[15] shows that an *undriven* molecule, which has relaxed into one dipole state, must overcome a barrier of about 68 meV to switch into the opposite state. The electronic localization is so great that level anticrossing is not resolvable. By the usual application of the Robin and Day classification scheme,[15] Figure 6 would suggest that **1** be considered a Type II system with reasonably strong localization and a significant barrier (>2 kBT) between states. Thermal fluctuations must provide the energy cost of nuclear reorganization.

(15) For a recent review of Robin and Day classes in mixed-valence chemistry see: Demadis, K. D.; Hartshom, C. M.; Meyer, T. J. *Chem. Rev.* **2001**, *101*, 2655.

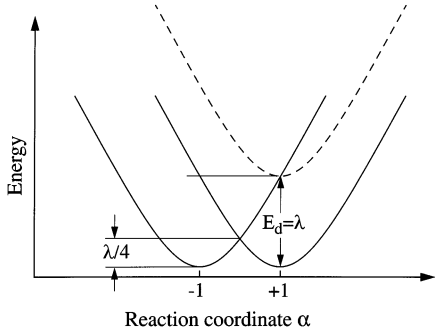

Figure 7. Schematic double-well potential and effect of a driver. The solid curves show the double-well potential when no driver is present. The dashed line shows the effect of an applied dipole driver, raising the energy of one parabola. If the driver is sufficient to raise the energy by λ, the reconfiguration energy, then no barrier exists for switching to the lower-energy state.

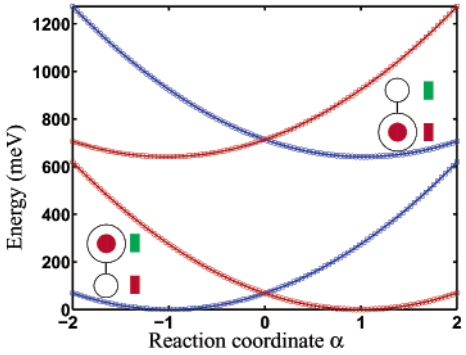

Figure 8. Calculated double-well potential in the presence of dipole driver. The blue curves correspond to the situation shown schematically in Figure 7. The driver has raised the energy for the electron occupying the lower dot. The dipole driver corresponding to the $m = 3.5$ e Å dipole of Figure 4d is sufficient to completely remove the barrier for relaxing to the low-energy state. Red curves correspond to a driver of opposite sign.

To understand QCA switching behavior, we must consider the response of the system to a driver. Figure 7 shows schematically the effect of an applied dipole driver. When the driver is off, the double-well diagram is comprised of two parabolas centered at the two relaxed charge configurations ($\alpha = +1$ and $\alpha = -1$) shown by solid lines in the figure. The barrier height in the absence of any state mixing (which we have seen is negligible here) is $\lambda/4$, where the direct excitation energy between the two configurations is λ. The effect of a dipole driver is to raise one parabola with respect to the other by an amount E_d. The dashed line shows the special case when the driver raises the energy of the PLUS configuration by an amount $E_d = \lambda$. When the effect of the driver reaches this level, the system can move between the metastable $\alpha = +1$ configuration and the new equilibrium $\alpha = -1$ configuration without having to surmount an energy barrier.

Figure 8 shows the energy-coordinate diagram for **1** when the system is driven with a dipole driver as described above. The blue (red) curves are for applied drivers with a positive (negative) dipole moment. The upper parabola in each case can be seen to be displaced upward to an energy 641 meV above the ground state. This is more than the direct reorganization cost ($\lambda = 472$ meV), so the transition from one state to the other proceeds with no barrier to surmount. The driver provides more than enough energy to overcome the reorganization cost.

It is important to note that the bistability relevant for QCA operation is the electronic bistability illustrated in Figure 5, and not that of Figure 6. The Robin and Day classification is not directly relevant. Indeed, the *frozen* symmetric geometry **1**-SYM which results in the bistability of Figure 5 would be represented as a flat line on the energy-coordinate diagram and be classified as Class III. Yet the QCA bistable switching behavior is still quite strong as evidenced by the abrupt switching shown in Figure 5. The point here is that Robin and Day classification relates to bistability, which results from the interaction of the nuclear motion with the electronic motion. This interaction can enhance or impede QCA function, but the bistability that QCA uses is fundamentally electronic and related to the effect of a driver potential; it could be present even if nuclear motion were entirely suppressed.

The bistability shown in Figure 6 illustrates a feature of molecular QCA that is not present in solid-state implementations. The bistable response of the electronic system is coupled to classical nuclear degrees of freedom. This adds another nonlinearity which has the effect of stabilizing the state through the self-trapping effect of nuclear relaxation, potentially enabling much longer memory times. On the other hand, it means that additional energy must be supplied to the system to overcome the barrier to switching. Fortunately, this energy is stored in the configuration of the molecular geometry and is therefore recoverable; that is, it need not be dissipated as heat. In the two-state molecule we examine here, the extra energy can only come from the driver. For large arrays, that will be insufficient. Molecular QCA will, therefore, finally require a clocking approach like that described by Toth et al.[16] for metal-dot QCA and by Hennessy and Lent[17] for molecules. This will entail using a molecule with three stable redox states. The third state could correspond to either occupation of another redox site or removing the unpaired electron from the molecule altogether. An external clocking field would provide the (recoverable) energy needed to surmount the reconfiguration barrier. That is, however, beyond the scope of the present work.

Electrostatic Description. A key energy for QCA is the so-called "kink-energy", which is the energy required to excite the molecule into a state with its dipole moment parallel to that of the driver. This can be viewed as the energy necessary to flip the bit into a "mistake" state. Our detailed calculations show that this energy can be well approximated by simple electrostatic models of single charges moving between effective charge centers within the molecule.

The calculated change in the dipole moment of the molecule under the action of the driver (Figure 5) is $\Delta\mu = 7.2$ e Å, corresponding to the movement of a unit charge a distance of 7.2 Å, which we can take to be the effective distance between the redox centers on the allyl end-groups. Note that this is not the same as the distance between any pair of atoms. A simple electrostatic calculation of the corresponding energy cost of the charge being in the "wrong" position (the molecular dipole aligned with the driver) yields a corresponding value of $E_{kink} = 622$ meV. The full calculation yields a value of $E_{kink} = 646$ meV for the frozen **1**-SYM geometry (upper curve in Figure 5b), $E_{kink} = 641$ meV for the molecule in the opposite state (**1**-PLUS or **1**-MINUS) with the appropriate relaxed nuclear coordinates (the vertical shift between blue curves in Figure

(16) (a) Toth, G.; Lent, C. S. *J. Appl. Phys.* **1999**, *85*, 2977. (b) Orlov, A. O.; Kummamuru, R. K.; Ramasubramaniam, R.; Toth, G.; Lent, C. S.; Bernstein, G. H.; Snider, G. L. *Appl. Phys. Lett.* **2001**, *78*, 1625.
(17) Hennessy, K.; Lent, C. S. *J. Vac. Sci. Technol., B* **2001**, *19*, 1752.

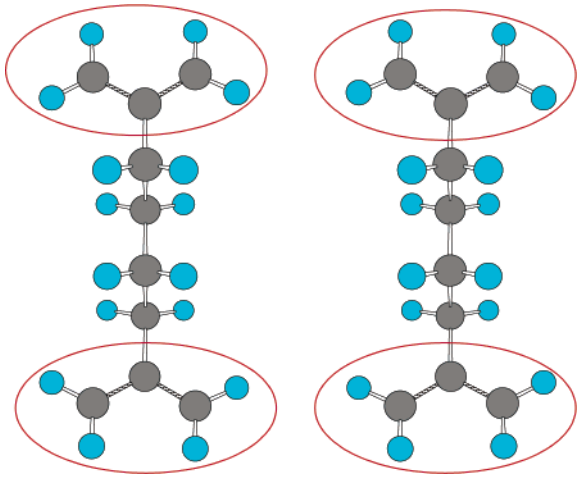

Figure 9. **2** is composed of two molecules of type **1**, arranged to make a roughly square cell. The dication of **2** is the molecular equivalent of the QCA cell shown schematically in Figure 1a.

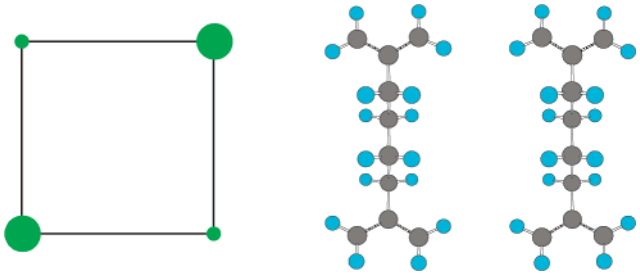

Figure 10. Geometry of the quadrupole driver used as input to **2**. The driver simulates the effect of another nearby molecular cell.

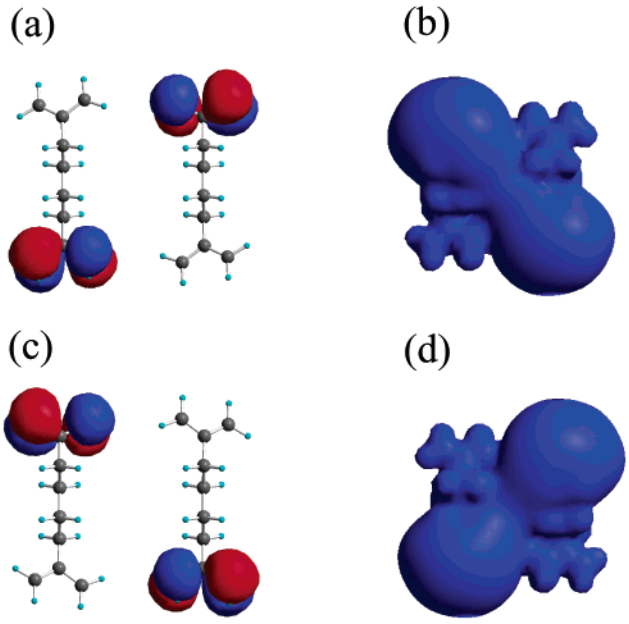

Figure 11. The HOMOs of the two stable states of the **2** dication are shown in (a) and (c). The corresponding isopotential surfaces ($V = 5$ au) are shown in (b) and (d).

6), or $E_{kink} = 555$ meV when the molecule is allowed to relax in the presence of the driver (lower curve in Figure 5b). This latter case is anomalous due to an artifact of the geometry – the molecule is driven on one side but not the other and therefore can lower its energy by flexing away from the driver. The agreement between the other ways of determining E_{kink} shows

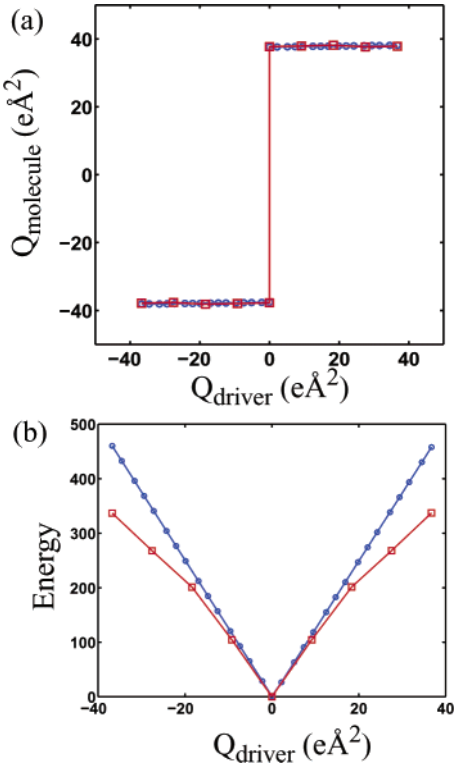

Figure 12. Molecular QCA response. (a) The response function of **2** when driven by a quadrupole driver as shown in Figure 10. For each driver quadrupole moment, the induced molecular dipole moment is calculated. Solid blue circles are for the case of a nuclear geometry frozen in the geometrically symmetric configuration. Red squares are obtained by letting the molecule relax to its equilibrium position in the presence of the driver. (b) The excitation energy (in meV) from the ground state to the first excited "mistake" state as a function of driver moment. Blue circles correspond to the frozen symmetric geometry, and red squares correspond to the relaxed geometry. The nonlinear bistable response is just what is required for QCA behavior. Furthermore, it is clear that the driver is switching the first (leftmost) molecule in Figure 10, and this molecule is in turn switching the rightmost molecule. The direct effect of the driver on the right molecule would be in the opposite direction.

that the kink energy is dominated by simple electrostatics and supports the efficacy of simple electrostatic models for a first-order description of QCA energetics.

Double-Molecule Response

We construct a double molecule by considering two molecules **1** arranged so that the charge centers on the allyl ends form an approximate square (the distance between the two molecular center lines is 7 Å). This double molecule, **2**, is shown in Figure 9. We can treat this as a single four-dot QCA cell or as a pair of QCA half-cells. The two central carbon atoms in each butyl bridge are again held fixed.[18]

Geometry optimization was performed on **2** through a procedure completely analogous to that described above. We consider the double-molecule dication and characterize the response of the double molecule by the quadrupole moment $Q_{molecule}$ evaluated about the molecular center. We employ a driver which consists of positive charges arranged on the corners of a square 7 Å away from the molecule as shown in Figure 10, mimicking the presence of another double molecule. The

(18) We again ignore the complications of attachment to a surface or to neighboring molecules, which would be necessary to realize a full molecular QCA system.

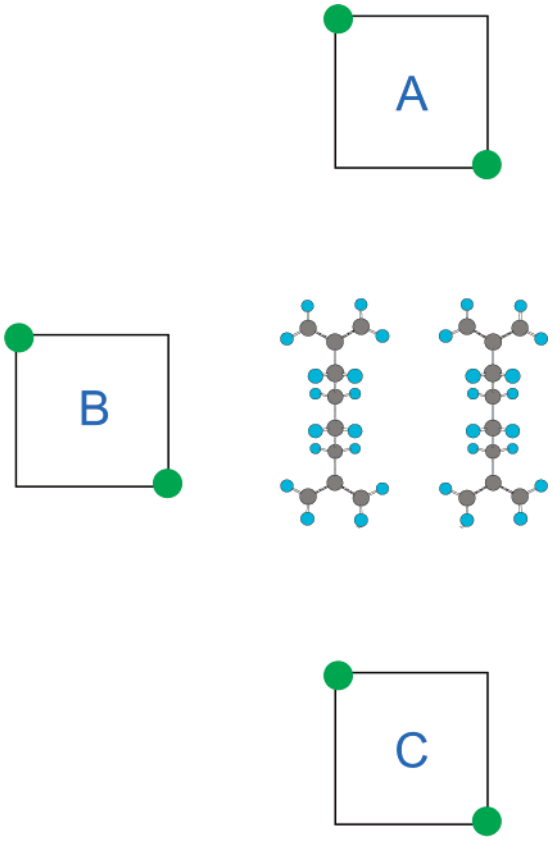

Figure 13. Geometry of a QCA majority gate using **2**. Inputs A, B, and C are quadrupoles which simulate the charge configuration of other QCA molecules.

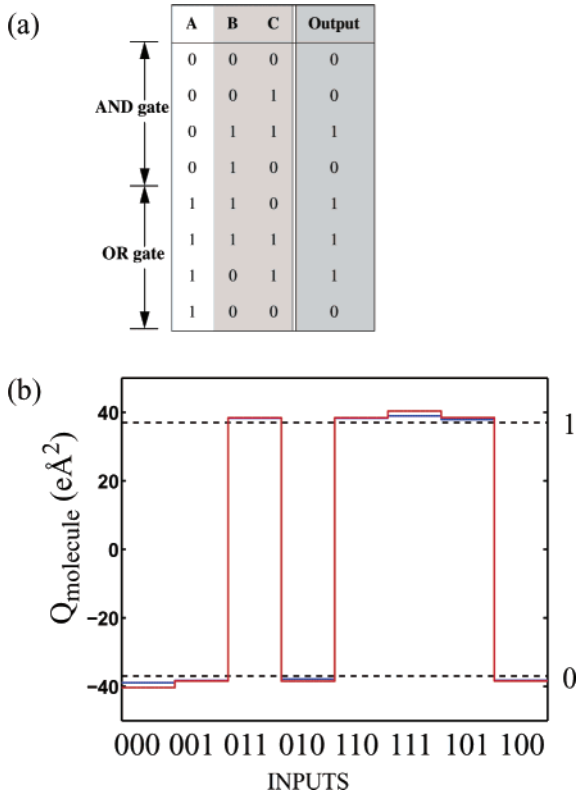

Figure 14. Molecular QCA majority gate. (a) The truth table for a three-input majority gate. (b) The calculated response of the molecular gate shown in Figure 13. For each of the eight possible input states, the ground-state molecular quadrupole moment was calculated. For both input and output, a bit value corresponds to the saturated values from Figure 12. A bit value of 1 (0) is represented by a quadrupole moment of 37.8 e Å^2 (−37.8 e Å^2). The blue line is for the case of a nuclear geometry frozen in the geometrically symmetric configuration. The red line is obtained by letting the molecules relax to their equilibrium positions in the presence of the driver.

magnitude of the positive driver charge on the four corners is varied smoothly to adjust the quadrupole moment of the driver Q_{driver}. The bit value stored in the double molecule can now be taken to be the sign of the molecular quadrupole moment.[19] The calculated quadrupole moment of 37.8 e Å^2 is precisely what would be expected from a simple electrostatic analysis of unit charges at the charge centers: $Q = (^3/_2)(3.5\ \text{Å})(3.6\ \text{Å}) = 37.8\ \text{e Å}^2$. The HOMO and potential surfaces are shown in Figure 11 for the two ground-state charge configurations.

The relevant QCA response function, shown in Figure 12a, is the induced molecular quadrupole moment as a function of the driver quadrupole moment. Points are calculated for both the case of frozen nuclear positions and the case where for each value of the driver quadrupole, the molecular configuration is allowed to relax. The self-trapping of the charge effected by the relaxation has a negligible effect on the response function. For electrostatic energy reasons, the quadrupoles of neighboring four-dot cells tend to align. This is the architectural advantage of four-dot cells over two-dot half-cells − it is not necessary to keep track of the number of cells in an inverter chain. Again, we see the strongly nonlinear bistable transfer characteristic. The excited state energy AE(Q_{driver}) (calculated as discussed above) is plotted in Figure 12b.

It is illuminating to consider the response of the double molecule considered as two single molecules in a chain with the driver. Note that the driver tends to push the closest (left-most) molecule into the correct state. Yet the direct effect of the driver on the second (right-most) molecule is opposite to what is required to flip the state. The second molecule flips its state because of the influence of the first molecule, not because of the direct effect of the driver. The driver influences the first molecule, which in turn influences the second. Thus, we see demonstrated the fundamental property needed for QCA operation: one molecule can exert enough influence over its neighbor to change its state.

(19) Note that the definition of cell polarization in ref 1 is precisely the normalized quadrupole moment.

Molecular Majority Gate

We use molecule **2** to model the molecular analogue to the three-input QCA majority gate, which has been demonstrated in the metal-dot QCA system. The geometry of the drivers for the majority function is shown in Figure 13. We use quadrupole drivers with a geometry and quadrupole moment chosen to mimic the behavior of the double molecule and solve for the molecular ground state. By stepping through the possible input combinations and finding the quadrupole moment of the molecular ground state for each one, we construct the calculated output characteristics of the molecular QCA majority gate. The results shown in Figure 14a are in full agreement with the required logical outputs displayed in the truth table of Figure 14b. The A input can be viewed as switching the functionality between (B and C) and (B or C). The A input is thus the program input for a programmable "and/or" gate. This represents the first

theoretical demonstration of a QCA logic gate at the molecular level.

Discussion

We have employed a simple model system to explore the possibilities of molecular QCA. Nonbonding orbitals, here in a π-system, are employed as "dots", redox centers among which unpaired electrons can distribute in more than one way. An alkane bridge provides a tunneling barrier between the two dots. The stable arrangements of charge among the dots are used to encode binary information.

We have explored the role of nuclear relaxation in the rearrangement of charge within the molecule. For the system considered, the electronic bistability is sufficient to enable QCA operation even in the absence of nuclear relaxation. Nuclear relaxation adds a self-trapping mechanism which may stabilize the bistability even more but is fundamentally distinguishable from it.

The electric fields associated with the flipping of a single molecular dipole are sufficient to drive neighboring molecular dipoles. Although molecular QCA will finally require clocked control, as in the metal-dot system, it is important that the strength of the coupling be shown to be adequate. Kink energies on the order of $^1/_2$ eV $\approx 20\ k_BT$ appear quite attainable, making thermodynamic mistakes quite rare. Using double or triple lines of cells would increase the kink energy further.

We emphasis that the molecule we have considered here is a model system, meant to capture some key QCA features, not a complete QCA implementation. The diallyl system lacks rigidity and has no attachment points for bonding to the surface. We have also considered the molecular cation and have not here dealt with the issue of the compensating charge, which could come from a counterion or an electrode. The electrostatics of this arrangement are key to any clocked QCA implementation.

We have provided a theoretical demonstration of a QCA majority logic gate operating at the single-molecule level. This provides an important example of a currentless, transistorless paradigm for molecular electronics.

Acknowledgment. This work was supported by the Defense Advance Research Projects Agency and the Office of Naval Research. The authors thank Prof. Thomas Fehlner for help and encouragement.

JA026856G